





Fantastic Scientific Agents and How to Build Them: AgentBuild for Rietveld Refinement

Woong Shin , Craig A. Bridges , Marshall T. McDonnell , and Rafael Ferreira da Silva 
Oak Ridge National Laboratory, Oak Ridge, TN, USA
{shinw, bridgesca, mcdonnellmt, silvarf}@ornl.gov

Abstract—As scientific workflows shift from deterministic executables to LLM-based agents, the development practices on offer, such as fine-tuning, reinforcement learning, and prompt-and-go, bury the scientist’s judgment. We propose treating agent construction as a workflow stage and introduce AgentBuild, which builds a scientific agent from a contract the scientist authors. The contract is a version-controlled rubric, a difficulty-graded curriculum, and a curated external knowledge base. A rubric-driven judge gates a meta-optimizer coding agent that edits the agent within a declared boundary, so the build compiles the agent, not the scientist’s judgment. We instantiate this for Rietveld refinement of X-ray diffraction data through GSAS-II behind MCP and A2A, where a blank-harness construction run progresses through a lithium lanthanum zirconium oxide (LLZO) signal-to-noise ladder, reaches the 4 hour scan as a frontier case, and exposes the workflow-scope limits that remain. The same rubric that rewards credible fits also scores trajectory scope, making the frontier a contract failure rather than a pattern-fitting failure. As base models evolve, re-running AgentBuild is a re-tune, not a rebuild, and the scientist’s authored contract remains the durable asset.

Index Terms—scientific workflows, agentic workflows, AI agent construction, eval-driven development, FAIR workflows, provenance, Rietveld refinement, X-ray diffraction

I. INTRODUCTION

Scientific workflow management systems [1] have spent two decades carrying deterministic executables across institutions and instruments, making “move a typed input through a sequence of fixed programs” a solved primitive. The agentic era breaks the underlying assumption. The executable at a workflow node is no longer a fixed program but a Large Language Model (LLM) agent whose prompts, tools, and code shift with every base-model release and scientific instrument upgrade. Off-the-shelf LLMs are not yet workflow-competent [2], so the open question is not whether to put an agent at a node but how to construct one, and how to construct it again when the base model changes next quarter.

The development practices on offer bury the scientist’s judgment where the scientist cannot reach it. Supervised fine-tuning encodes domain expertise into weights that are not

legibly diffable and do not survive a model swap. Reinforcement learning (RL) with verifiable rewards [3], [4] adds a further demand for a clean scalar reward, which the visual, multi-criterion judgments that scientists actually make do not reduce to. Prompt-and-go wiring of a base model avoids both problems but offers no acceptance bar in their place. Across all three, you cannot find the agent in any of the usual places, and the scientist is left without a legible artifact that indicates what a competent analysis looks like.

The agent’s domain competence originates in the scientist’s distilled judgment, and this paper’s contribution is a way to keep that judgment legible, authored, and outside the build loop. We treat the judgment as a three-part contract authored by the scientist. A version-controlled rubric states the qualitative and visual criteria a competent analysis must satisfy. A difficulty-graded curriculum pairs representative samples with reference reports. A curated external knowledge base distills the procedures on which the domain relies. The scientist’s role is authoring, not agent-coding, and the build compiles the agent, not the scientist’s judgment. This is the non-replacement guard: a base model can help format the authored artifacts, but the rubric and the curriculum constitute the scientific claim, and the scientist owns them.

In this paper, our contributions are as follows:

- **An agent-construction methodology** that locates an agent’s domain competence in the scientist’s authored contract and assigns the scientist an authoring role rather than an agent-coding role. Section IV grounds it in the SNR experiment, where a blank-harness construction run progresses through a lithium lanthanum zirconium oxide (LLZO) signal-to-noise (SNR) ladder, meaning the same LLZO powder pattern measured at progressively longer count times, under the authored rubric. Specifically, X-ray powder diffraction data were collected on a Ta-doped Li-ion conducting solid electrolyte based upon LLZO.
- **AgentBuild, a workflow stage** that compiles the agent from that contract. The stage exposes a declared interface, a rubric-driven LLM-as-judge acceptance test, a meta-optimizer that mutates the multi-component agent assembly (including, case by case, the tool layer), and a provenance-tracked output whose interface persists across model swaps. Together these properties distinguish it from prompt-only optimizers and single-artifact program-search systems (Section V), and the durable-interface property is grounded at the artifact level in Section II.

This manuscript has been authored in part by UT-Battelle, LLC, under contract DE-AC05-00OR22725 with the US Department of Energy (DOE). The publisher, by accepting the article for publication, acknowledges that the U.S. Government retains a non-exclusive, paid up, irrevocable, worldwide license to publish or reproduce the published form of the manuscript, or allow others to do so, for U.S. Government purposes. The DOE will provide public access to these results in accordance with the DOE Public Access Plan (<http://energy.gov/downloads/doe-public-access-plan>).

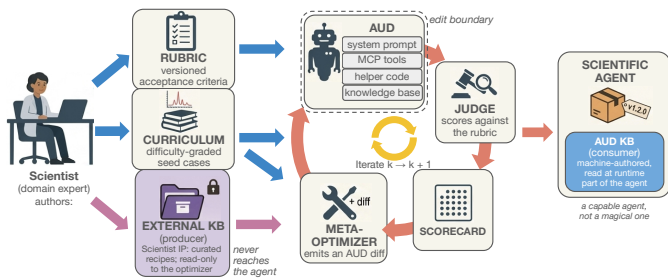


Fig. 1. The AgentBuild loop. The scientist and the three authored artifacts (the version-controlled rubric, the difficulty-graded curriculum, and the curated external knowledge base) are the loop’s left-hand origin; the rubric-driven judge scores each curriculum case into a scorecard that gates the meta-optimizer build step in the center; and the Agent-Under-Development (AUD) emerges on the right as a versioned, A2A-packaged box carrying its own machine-authored consumer knowledge base.

- **A Rietveld and X-ray diffraction (XRD) case study** driving GSAS-II [5] through a Model Context Protocol (MCP) server [6] behind A2A [7]. The case study gives each clause of the contract concrete evidence (Section IV).

Together they answer where a scientific agent comes from, how it is built, and what it is once built. The remainder of the paper develops this in three acts. Section II presents AgentBuild as a workflow stage, opening on the scientist-authored artifacts before the build mechanism that consumes them. Section III instantiates the stage for Rietveld refinement on GSAS-II. Section IV reports the SNR construction trajectory, the rubric contract, and the 4 hour frontier that separates credible fitting from strict workflow-scope success. Section V positions the methodology against the agent-construction and self-driving-science lineages, Section VI concludes.

II. AGENTBUILD: A WORKFLOW STAGE PRIMITIVE

AgentBuild is a scientific workflow stage whose job is to construct an LLM-based agent for execution at a later stage of the same or a federated workflow. A workflow stage is composable, with a declared interface, a body of work it performs, and a typed output other stages consume. The agent’s procedural competence lives in the scientist’s authored contract. In this Section, we outline the three artifacts the scientist authors before describing the build mechanism that consumes them. Figure 1 shows the loop end to end. The scientist and the three authored artifacts on the left are its origin, the rubric-driven judge and the meta-optimizer build step run in the center, and the agent emerges on the right as a packaged box.

A. Three authored pillars

The scientist authors three pillars, and they are the concrete answer to where the agent’s domain competence comes from. The first is a version-controlled *rubric*, a specification of the qualitative and visual criteria the agent’s outputs and trajectories must satisfy, with strict pass thresholds on every dimension. The rubric is the testable artifact that captures the

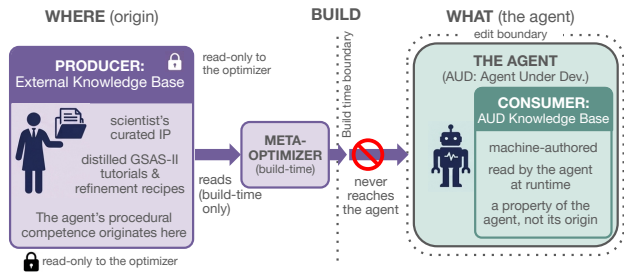


Fig. 2. The two-knowledge-base seam. The producer external knowledge base (purple) is the scientist’s curated intellectual property, read by the meta-optimizer at build time and blocked from crossing into the agent. The consumer AUD knowledge base (teal) is machine-authored, lives inside the agent, and is read at runtime. The producer knowledge base is the agent’s origin and never becomes part of the agent.

domain expert’s judgment in legible, author-attributed form. The second is a difficulty-graded *curriculum*, a set of paired tuples in which each tuple is a representative scientific sample plus a reference report of what a competent analysis of that sample looks like, arranged from easy to hard. The third is a curated *external knowledge base*, distilling the procedures the domain relies on, authored by the scientist as the source the build draws procedural competence from. Section III populates all three pillars concretely for Rietveld refinement, with the rubric dimensions and thresholds enumerated in Table II.

B. Two knowledge bases

AgentBuild keeps two knowledge bases distinct so the final knowledge distillation can be specific and tailored to the underlying model capability. The *producer external knowledge base* is the scientist’s curated, read-only corpus. The meta-optimizer reads it at build time, and it never crosses into the agent. It remains the scientist’s intellectual property and is the place the procedural competence originates. The *consumer AUD knowledge base* is machine-authored, lives inside the agent’s edit boundary, and is read by the Agent-Under-Development (AUD) at runtime. It is a property of the built agent, not of its origin.

Figure 2 renders the boundary. The producer knowledge base (purple) is read-only to the meta-optimizer and blocked from reaching the agent, while the consumer AUD knowledge base (teal) sits inside the agent.

C. Stage contract

The AgentBuild contract has six declared inputs, one acceptance test, one build step, and two outputs, with a promotion gate that releases a candidate. Figure 3 traces the loop end to end. The scientist-authored inputs sit at the top-left origin, the build step runs downstream, and the versioned output and provenance trail exit on the right.

Declared inputs. The first declared input is the *curriculum* and the second is the *rubric*, both described above. The third is the *producer external knowledge base*, the scientist’s curated, read-only procedural source for the build. The fourth is a *base model handle* that names the specific LLM checkpoints

used by the AUD, the judge, and the meta-optimizer. The fifth is an *MCP tool inventory* [6], the set of Model Context Protocol primitives the AUD may invoke, exposed by an MCP server that fronts the scientific engine. The sixth is the *edit boundary*, a table declaring which surfaces of the AUD assembly the meta-optimizer may mutate (system prompt, tool wiring, helper code, and, case by case, the MCP server code) and which are frozen for the duration of a build (the underlying engine, the curriculum, the rubric, the producer external knowledge base, and the judge scaffolding).

Acceptance test. The acceptance test is a rubric-driven LLM judge that scores the AUD’s trajectory on each curriculum case along the rubric’s output and trajectory dimensions; Table II gives the Rietveld instantiation used in this manuscript. Per-case scoring aggregates into a per-iteration verdict. This is the LLM-as-judge methodology [8] cast as the stage’s typed acceptance test rather than as a free-standing evaluation harness. The convergence criterion is the pass criterion *P-strict*. In the same iteration, the judge’s scores meet all thresholds across every rubric dimension for every active curriculum case. *P-strict* and the event-driven tier-escalation rule in which a tier is added when the AUD passes the prior tier under *P-strict*, are the pre-registered acceptance bar, declared here before any results so the band is fixed independent of what the build produces.

Build step. The build step is a meta-optimizer LLM that mutates the AUD assembly within the edit boundary, conditioned on the judge’s last verdict and the curriculum’s current frontier. The search target is the AUD assembly itself, not a single program or a single reward function. Prompts, tool wiring, helper code, and, when the boundary permits, the MCP server glue are co-edited. The build step’s invariant is end-to-end executability after every mutation. Each candidate AUD must run through the curriculum without crashing, regardless of its score.

Provenance-tracked output. The promotion gate is rubric saturation under *P-strict* plus a release tag. When it fires, AgentBuild emits two outputs. The primary output is a versioned, A2A-packaged AUD [7], deployable behind a well-known URI without re-authoring the orchestration layer. The secondary output is a *provenance trail* covering the rubric and curriculum versions, every meta-optimizer diff against the AUD, every judge transcript, every model handle, and every tool version that participated in the build. The provenance trail is what makes the FAIR-CWFR position [9] reachable for agents built by workflows since the construction is itself a workflow whose run serializes as PROV [10] and pools with other runs against the FAIR Principles [11] and FAIR for Research Software [12].

D. Durable interface

The interface AgentBuild declares what persists across model generations beyond a single instantiation. When the base model handle changes, re-running AgentBuild against the same rubric and curriculum is a re-tune rather than a rebuild. The rubric and curriculum are the project’s intellectual asset,

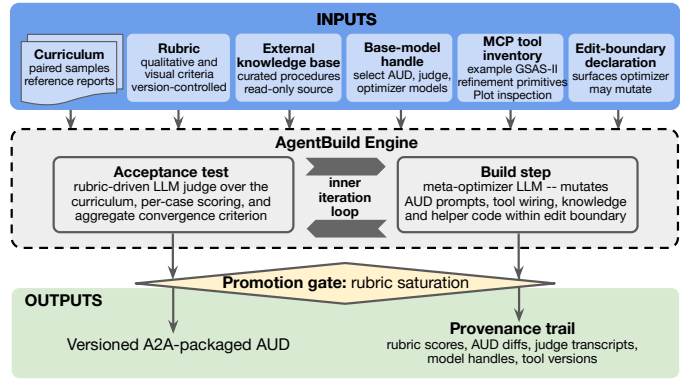


Fig. 3. The AgentBuild stage contract. The six declared inputs (curriculum, rubric, base model handle, MCP tool inventory, producer external knowledge base, edit boundary) occupy the top-left origin, the rubric-driven judge and the meta-optimizer build step form the inner loop, and the promotion gate releases a versioned A2A-packaged AUD and a provenance trail on the right. The scientist-authored inputs sit upstream of the build step, and the left-to-right ordering is the methodology’s origin-then-build sequence.

TABLE I
FAIR COVERAGE OF THE AGENTBUILD CONSTRUCTION-SIDE ARTIFACTS.
● MARKS THE PILLAR AN ARTIFACT MOST DIRECTLY REALIZES AND ◐ A PILLAR IT PARTIALLY SUPPORTS

Construction artifact	F	A	I	R
Rubric + curriculum (authored contract)	◐		◐	●
A2A-packaged AUD endpoint	◐	●	◐	
Typed stage contract / agent card	◐		●	
Meta-optimizer diff trail (PROV)	◐	◐	◐	●

and the A2A-packaged AUD is a derivative any sufficiently capable base model can re-derive against the same interface. When the handle flips from one checkpoint to a successor, the rubric specification, the curriculum records, the MCP tool inventory, the judge scaffolding, and the workflow DAG that calls AgentBuild are all unchanged. What changes is the AUD’s internal prompts and helper code, recorded as a new provenance entry tagged with the new handle. The A2A endpoint contract presented downstream remains identical. Agents built by workflows can only be as FAIR as the trail that constructed them, so an agentic node’s FAIRness must cover the rubric that defined acceptance, the curriculum that defined the regression suite, and the meta-optimizer diff trail that produced the deployed agent. The four construction-side artifacts map onto the FAIR-CWFR pillars [9], [13], as Table I summarizes.

This durable-interface property is a key reinforcing limb of the methodology. “How to build the agent” and “what survives a model swap” are the same property seen from two ends, since the build is cheap to re-run precisely because the authored contract is durable. This property distinguishes AgentBuild from supervised fine-tuning, reinforcement learning with verifiable rewards [3], [4], and foundation-model training, all of which bury the expert’s judgment in parameters that do not survive a model swap or an upgrade. AgentBuild keeps

that judgment in an author-attributed rubric specification and curriculum records. The non-replacement principle follows as a design choice rather than an incapacity claim, since the rubric’s authorship constitutes the scientific claim of the workflow and co-authoring it with a base model would put the claim’s authority at risk.

E. Inner discipline, composition, and non-goals

AgentBuild’s inner discipline is evaluation-driven development plus curriculum learning plus mutation-and-selection search. The rubric supplies the typed acceptance signal, the curriculum supplies the graded difficulty schedule, and the meta-optimizer supplies the discrete search step over the AUD assembly. Adjacent agentic primitives such as ReAct [14] and Reflexion [15] operate inside a single running agent’s read-write surface, modifying in-context memory, whereas AgentBuild modifies the agent *artifact* (prompts, tools, code) and packages the result as a deployable A2A agent. The typed A2A endpoint and provenance trail are consumed by a host workflow in its native idiom, so Pegasus [16], Snakemake [17], Nextflow [18], CWL [19], Parsl [20], funcX [21], and Galaxy [22], [23] each receive AgentBuild as a typed stage, and the same DAG replays against a swapped handle without re-authoring.

Three properties distinguish AgentBuild from prompt-only optimizers (DSPy [24] and GEPA [25]) and single artifact program-search systems (FunSearch [26], Eureka [27]). The MCP server sits inside the edit envelope case by case rather than being frozen, the acceptance criterion is a rubric-driven LLM judge over visual and textual dimensions rather than a scalar metric, and the output is an A2A-packaged container with a typed contract and a provenance trail rather than an in-process module. Section V develops the comparison.

AgentBuild is not a benchmark, a chat wrapper, an end-to-end autonomous-discovery system, or a replacement for the expert. It is a workflow stage whose contract converts a capable base model plus an expert’s rubric and curriculum into a deployable, provenance-tracked, A2A-packaged agent. With this instantiation, we leave identity propagation through MCP tool chains, A2A endpoint multi-tenancy, rubric exploitation under adversarial pressure, and curriculum bootstrapping in domains without an authored seed as workflow-system future work.

III. RIETVELD REFINEMENT VIA GSAS-II

In this Section, we apply AgentBuild in the context of building an scientific agent that does Rietveld refinement with the intent of using it as a building block for autonomous science. Rietveld refinement is whole-pattern least-squares refinement of a crystallographic model against measured powder diffraction data [28]. The method is robust against peak overlap, as the overlap is continuously evaluated as a refinement proceeds, and it allows for important structural parameters (e.g., lattice parameters, atomic positions) and microstructural parameters (e.g., crystalline domain size or lattice strain) to be extracted from the data on crystalline powders. This method is difficult

to fully automate because its standard metric fails bidirectionally. The refinement fits a physically motivated forward model (crystal structure, sample microstructure, instrument profile, background) to the measured pattern and reports a weighted profile R-factor (Rwp) at convergence, typically 5 to 15 percent on laboratory data. Rwp can be locally favorable while the rendered pattern visually disagrees with the data, and a physically correct fit can read as higher-Rwp than a near-degenerate competitor; the noise level and the possible presence of impurities particularly complicate the fit evaluation solely based upon Rwp. Expert crystallographers therefore treat visual inspection of the rendered pattern, not Rwp in isolation, as the gold standard for accepting a refinement which makes Rietveld refinement particularly difficult to fully automate without human intervention. We tackle this issue by designing an AI agent with a visual inspection driven loop by leveraging the visual reasoning capabilities of frontier LLM based models such as Claude Sonnet and Opus from Anthropic [29].

A fully autonomous Rietveld refinement agent enabled by AgentBuild is ideal for deployment in settings for which immediate and autonomous feedback from Rietveld refinement is crucial for accelerating experimental operation. This enables autonomous chemistry laboratories or insitu/operando studies at neutron/synchrotron facilities, but could also transform the data analysis protocol for any laboratory X-ray diffraction data collection. One example is deployment in the Autonomous Chemistry Laboratory (ACL) at ORNL [30]–[32], which contains robotic synthesis tools developed as part of the ORNL INTERSECT project [33] for dispensing and manipulating liquids and solids for both organic and inorganic solid-state chemistry. The ACL contains custom in-house solutions for high energy milling powder mixtures, transferring powders to and from crucibles, and reacting powders at high temperature to form compounds such as LLZO. An integrated online X-ray diffractometer can provide XRD data for automated agentic analysis with the workflow we report here, better enabling closed-loop workflows for solid-state synthesis.

A. Contract for Rietveld Refinement

The six declared inputs of the AgentBuild contract in the context of Rietveld Refinement are populated as follows. The *curriculum* uses a difficulty-graded signal-to-noise (SNR)

TABLE II
RUBRIC DIMENSIONS AND P-STRICT THRESHOLDS FOR THE SNR EXPERIMENT.

Code	Dimension	Contract checked	Pass
D1	Phase ID	Correct phases and groups; no false positives.	✓ 3
D2	Quant. agreement	Fractions meet major/minor tolerance bands.	✓ 3
D3	Fit indices	Fit metrics present, parseable, plausible.	✓ 3
D4	Chemistry	Chemistry and refined effects remain plausible.	✓ 2
D5	Uncertainty	Limits, alternatives, confidence stated.	✓ 2
D6	Report structure	Report elements, plot reading, tone present.	✓ 2
T1	Workflow order	Limits/background before profile/atoms.	✓ 3
T2	Tool use	GSAS-II choices fit data protocol.	✓ 3
T3	Recovery	Divergence detected, diagnosed, recovered.	✓ 2
T4	Efficiency	No redundant or circular operations.	✓ 2
T5	Visual feedback	Full/zoom plots inspected and acted on.	✓ 3

ladder. Its LLZO axis uses one $\text{Li}_{6.4}\text{La}_3\text{Zr}_{1.4}\text{Ta}_{0.6}\text{O}_{12}$ sample (MTI Corp., 99.99 percent) across count times, so the difficulty change is data quality rather than new chemistry. The domain-scientist rationale identifies this material as a strongly scattering Ta-doped cubic garnet (space group $\text{Ia}\bar{3}\text{d}$): short scans require constrained models with few variables, while the 4 hour scan can reveal a weak impurity contribution and justify a broader refinement envelope. That asymmetry is the reason the series is useful for AgentBuild. A correct AUD should not simply release more parameters as the case label becomes harder; it must match the refinement freedom to the information present in the pattern. The lowest-count scans test whether the agent can preserve chemically plausible constraints under noise, whereas the highest-count scan tests whether it can recognize that more structure is now visible without escaping the declared workflow protocol. The PXRD data were collected from the same commercial powder in air on a Malvern Panalytical Empyrean diffractometer with $\text{Cu K}\alpha$ radiation and a reflection-transmission stage with a zero background holder, covering 10° to 120° 2θ at 0.013° steps, with count times spanning 1 m 27 s, 3 m 38 s, about 10 min, 30 min, 1 h, and 4 h. The construction run begins with PbSO_4 and fluoroapatite baselines derived from GSAS-II tutorials, then adds the LLZO scans. The complete judged record introduces the LLZO 1 minute and 30 minute cases before reaching the 4 hour scan as a frontier case. The *rubric* is version-controlled; Table II enumerates its six output dimensions, five trajectory dimensions, and strict pass thresholds. The *producer external knowledge base* is the scientist’s distilled GSAS-II tutorials and refinement recipes, read by the meta-optimizer at build time and blocked from the AUD. The *base model handle* pins Claude Sonnet 4.6 as the AUD model and Claude Opus 4.7 as the judge-scoring and meta-optimizer model. The *MCP tool inventory* [6] exposes GSAS-II refinement primitives (peak fitting, phase addition, parameter refinement, residual computation) plus a `get_pattern_plot` primitive that renders the calculated pattern over the experimental data. A companion zoomed-plot primitive clips the same observed, calculated, and difference curves to a chosen 2θ window, so the AUD can inspect localized residuals and weak peak regions against the same visual evidence the expert uses. The *edit boundary* is the surfaces of Table III. The scientist authored all three pillars, and the build wrote the AUD, with the judge and meta-optimizer both based on Claude Opus 4.7.

B. Build topology

The AUD is a single-agent assembly on Claude Sonnet 4.6. Its three in-envelope surfaces (system prompt, tool wiring, helper code) implement an inner ReAct-style loop [14] that interleaves reasoning with tool invocation. GSAS-II [5], the open-source Rietveld engine, is exposed through an MCP server, which lets the tool layer remain fixed across AUD base-model swaps. The `get_pattern_plot` primitive is the key piece for the visual evidence required by Table II. It renders the calculated pattern over the observed pattern, returns the image to the AUD, and lets the AUD reason over the rendered

TABLE III
EDIT-BOUNDARY ENUMERATION. IN-ENVELOPE SURFACES ARE THOSE THE META-OPTIMIZER MAY MUTATE BETWEEN ITERATIONS, AND OUT-OF-ENVELOPE SURFACES ARE FROZEN FOR THE DURATION OF A BUILD. THE MCP SERVER IS IN-ENVELOPE CASE BY CASE; THE OPTIMIZER MAY ESCALATE TO THE SERVER-SIDE ADAPTER WHEN A RUBRIC CONTRADICTION LOCALIZES THERE, BUT THE GSAS-II CORE STAYS FROZEN.

Surface	Owner	Envelope
AUD system prompt	meta-optimizer	in
AUD-side tool wiring	meta-optimizer	in
AUD-side helper code	meta-optimizer	in
MCP server adapter	meta-optimizer	in (case-by-case)
MCP plotting helper	meta-optimizer	in (case-by-case)
Consumer AUD knowledge base	meta-optimizer	in
GSAS-II core	upstream project	out
Rubric specification	domain author	out
Judge prompt scaffolding	framework author	out
Curriculum tuples	curriculum author	out
Producer external knowledge base	domain author	out
Base model handle	operator	out

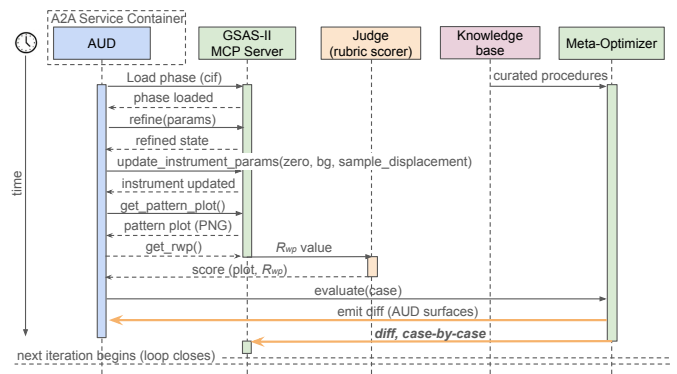


Fig. 4. The Rietveld build topology for one iteration. The Claude Sonnet 4.6 AUD, inside an A2A service container, drives GSAS-II through the MCP server (refinement primitives plus full-range and zoomed pattern plots), the rendered pattern returns to the AUD, the trajectory and the rendered pattern go to the Claude Opus 4.7 judge, and the meta-optimizer emits a case-by-case diff over the AUD surfaces. The producer external knowledge base is read at build time and does not cross into the AUD. The visual-evidence round trip, rendered pattern images returning to the AUD, is the call path on which the rubric’s visual-fit dimensions depend.

visual the way an expert crystallographer would. Its zoomed companion turns that feedback from a single global diagnostic into an active inspection loop over selected 2θ regions. The judge runs two passes against each iteration’s trajectory. A screening pass flags crashes and missing reports, and a scoring pass assigns the rubric scores listed in Table II, conditioned on the rendered pattern. The meta-optimizer receives the per-case verdicts, the trajectory, and the edit boundary, and emits a diff against the AUD assembly, with the executability invariant of Section II-C upheld and the diff recorded in the provenance trail. When the AUD passes on the active curriculum, the promotion gate fires and emits an A2A-packaged container with a well-known URI and an agent card. Figure 4 traces the call topology of one iteration.

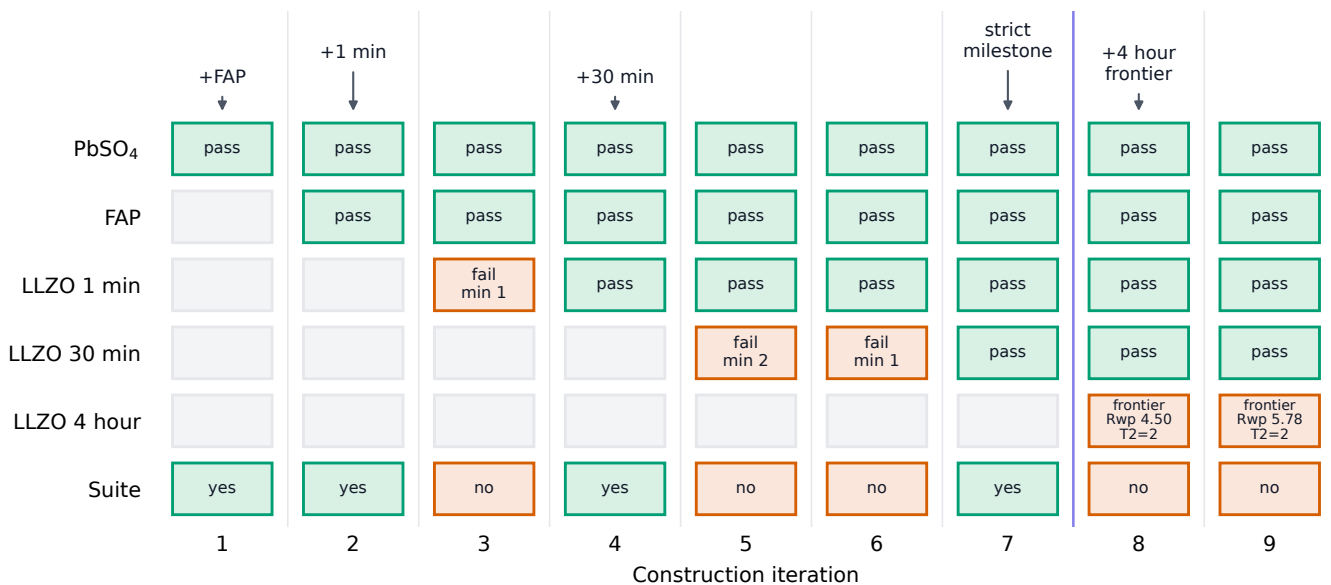


Fig. 5. Run-derived SNR construction trajectory. Iteration 7 is the last complete four-case P-strict milestone and triggers escalation to the 4 hour LLZO scan. Iterations 8 and 9 continue the same matrix with LLZO 4 hour as a normal trajectory row. Those cells show that the AUD reached plausible 4 hour fits, but the strict workflow-scope contract was not satisfied, so the 4 hour row is not a strict pass.

C. Pre-registered pass criterion

The acceptance criterion declared here, before any results, is *P-strict* of Section II-C, applied to the eleven rubric dimensions and thresholds in Table II. In a single iteration, every active curriculum case must meet every dimension threshold. Section IV therefore reports construction milestones and frontier failures as dimension-level evidence rather than a benchmark neighborhood or dominance claim.

IV. EVALUATION

The Rietveld evaluation uses a single SNR-focused construction experiment. The build starts from a blank AUD harness and a fixed AgentBuild contract for GSAS-II refinement. The active curriculum begins with PbSO₄ and fluorapatite baselines, then adds an LLZO signal-to-noise ladder: the same LLZO sample measured at progressively longer count times. The rubric, curriculum policy, tool inventory, judge, and meta-optimizer settings remain fixed across the judged construction iterations. No additional construction run was performed.

A. Experiment setup

The experiment instantiates the architecture of Section III. The AUD runs on Claude Sonnet 4.6, the judge screens on Claude Sonnet 4.6 and scores on Claude Opus 4.7, and the meta-optimizer runs on Claude Opus 4.7. The pass criterion is *P-strict* of Section II-C, applied the rubric dimensions of Table II. Escalation is event-driven. A new case is added only when the active suite passes under *P-strict*.

Table II in Section III-A makes the pass rule explicit. D1-D3 are deterministic checks on phase identity, quantitative agreement, and fit-index accountability. D4-D6 judge whether

the final report is scientifically reasonable and complete. T1-T5 judge the refinement trajectory itself. *P-strict* passes only when every active case clears every listed threshold in the same iteration, so low Rwp alone cannot satisfy the contract.

The executed protocol has two measured parts. The construction run measures how far a blank-harness build progresses through the LLZO count-time ladder under *P-strict* escalation. The holdout run applies the terminal AUD to reserved SNR cases that were not active during construction.

B. Results

The construction run progresses through the active SNR ladder before reaching its current frontier. Iterations 1 and 2 pass the initial single-phase baselines. Iterations 3 through 7 build toward the LLZO SNR cases. The key construction milestone is iteration 7, where the active four-case suite passes under *P-strict* and escalates to the 4 hour LLZO scan. The milestone is important because the same rubric, curriculum, tool inventory, and judge contract remain fixed while the AUD surfaces change.

Iterations 8 and 9 add the 4 hour LLZO scan. Four of five active cases pass per-case strict scoring in each iteration, but the 4 hour LLZO row fails the T2 workflow-scope dimension. The iteration 9 report on 4 hour LLZO gives a plausible refinement with Rwp 5.78%, Rp 4.54%, and RF 9.86%. The same report releases profile and atomic groups outside the constrained SNR protocol, so the run records a plausible fit without a strict workflow-scope pass.

Figure 6 shows the same boundary in pattern space. It compares the domain-scientist reference and the AUD final state for the iteration 7 construction milestone and the iteration 9 4 hour frontier. The panels are rendered from stored numeric

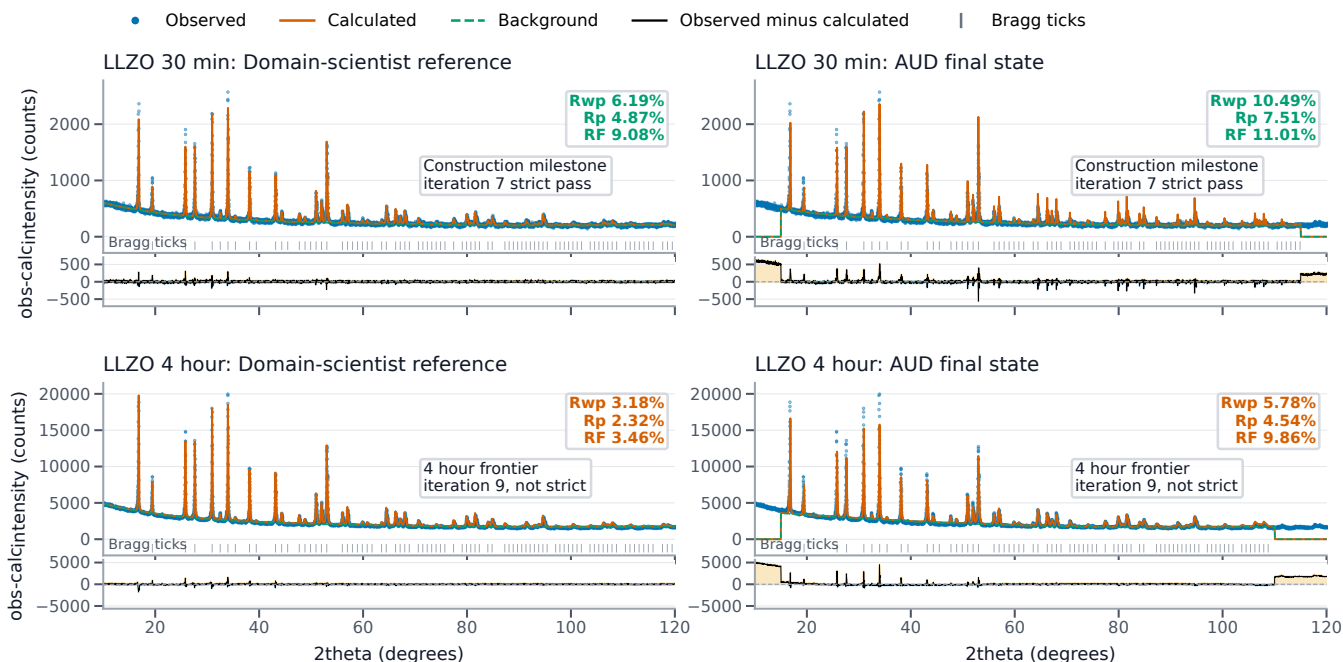


Fig. 6. Numeric Rietveld pattern evidence for the construction milestone and the 4 hour frontier. The top row is the LLZO 30 minute construction milestone, where the iteration 7 active suite passes under P-strict. The bottom row is the LLZO 4 hour frontier, where the iteration 9 AUD final state gives a plausible fit but remains outside the strict workflow-scope contract. Each row compares a domain-scientist reference panel with an AUD final-state panel rendered from stored numeric arrays, including observed, calculated, background, residual, and Bragg-tick arrays.

arrays, and the two rows use the same observed, calculated, background, residual, and Bragg-tick grammar.

The SNR holdout rows in Table IV test the same count-time axis as the construction curriculum.

The key row is the 10 minute LLZO holdout case. Its report gives Rwp 14.93%, Rp 10.86%, and RF 20.36%, identifies a single-phase cubic LLZO refinement, and discusses low-count limitations, microabsorption, and unresolved alternatives. Strict scoring fails D1-D3, while D4-D6 and all trajectory dimensions score at least 4.

C. Findings and limitations

The principal result is that AgentBuild constructs a usable Rietveld AUD from a fixed scientist-authored contract. The AUD is not hand-written by the scientist; it is produced by an iterative build stage that keeps the rubric, curriculum, tool inventory, and judge contract fixed while the agent assembly changes. The iteration 7 milestone is the evidence. The active four-case suite passes under P-strict and the run escalates to

the 4 hour LLZO scan. Iterations 8 and 9 then show that the constructed AUD can reach plausible high-count LLZO refinements.

The SNR holdout rows reinforce the same pattern while surfacing a practical lesson about machine-checkable reporting. The 3 minute and 1 hour rows pass, and the 10 minute row keeps strong D4-D6 scientific-reporting scores and strong trajectory scores. Its D1-D3 misses are best read as deterministic reporting-interface issues, not as evidence against the underlying refinement reasoning: phase accounting, fit-metric reporting, and reference-policy obligations must be expressed in forms that a deterministic checker can consume. That interface is surprisingly challenging because it is the front line where non-deterministic scientific narration first meets deterministic validation. Future builds should make that report contract more explicit and improve the parser-facing conventions around it.

The remaining limitations define the next expansion targets. This work evaluates single-phase, SNR-focused Rietveld refinement. It does not establish performance on phase identification, multiphase refinement, phase-count detection, weak impurity modeling, or broader material and instrument classes. Extending AgentBuild to those settings should mean expanding the rubric, seed curriculum, MCP tool surface, and edit-boundary table rather than simply reusing the SNR contract unchanged.

TABLE IV
SNR HOLDOUT ROWS.

Case	Strict	D1-D3	D4-D6	Interpretation
3 min	pass	5,5,5	5,5,5	Low-count pass; Rwp is SNR-limited.
10 min	no pass	1,1,1	5,5,5	D1-D3 fail; D4-D6 stay strong.
1 h	pass	5,5,3	5,5,5	Pass; D3 remains borderline.

V. RELATED WORK

Workflow and autonomous-science substrates. Pegasus [16], Snakemake [17], Galaxy [22], [23], Nextflow [18], CWL [19], Parsl [20], and funcX [21] provide the workflow substrates AgentBuild can compose with. FAIR-CWFR [9] specifies FAIR workflow-component properties [11]–[13], while PROV-AGENT [10] and the workflow-provenance agents of Souza et al. [34] address how agents and provenance interact. Campaign-scale autonomous systems, including ChemOS 2.0 [35], MADSci [36], Colmena [37], science factories [38], ChemCrow [39], autonomous chemistry agents [40], [41], and the AI co-scientist [42], operate experiments and discovery loops. AgentBuild is complementary: it constructs or refreshes the tool-facing agent artifact that such workflow and campaign substrates may call.

Agent construction and optimization. FunSearch [26] and Eureka [27] use LLMs as mutation operators over programs or reward functions, and AI Scientist [43] extends agentic search toward end-to-end research loops. DSPy [24] and GEPA [25] optimize prompts and demonstrations; ReAct [14] and Reflexion [15] shape in-context behavior inside a running agent; and reinforcement learning with verifiable rewards, including DeepSeek-Math [3] and DeepSeek-R1 [4], changes model weights around scalar or checkable rewards. These systems optimize programs, prompts, demonstrations, in-context state, rewards, or weights. AgentBuild instead constructs a deployable, tool-facing AUD assembly under a scientist-authored rubric, curriculum, knowledge base, and edit boundary.

XRD and Rietveld automation. GSAS-II [5] is the canonical open-source Rietveld engine AgentBuild drives. Ozaki et al.’s BBO-Rietveld work [44], which uses the Optuna library [45] for Bayesian optimization, is the closest published automation reference point. Methodology-wise, BBO-Rietveld optimizes refinement parameters, while AgentBuild constructs and evaluates the tool-facing AUD itself. XRD-AutoAnalyzer [46], the Crystallography Companion Agent [47], and Dara [48] cover adjacent automation at the phase-identification and pattern-interpretation layers. None frame the construction of the Rietveld-driving agent itself as an auditable workflow stage with a declared interface and a provenance trail.

VI. CONCLUSION

The scientific agents a workflow node runs are capable, not magical, and this paper shows where to find them and how to build them. They originate in the scientist’s distilled judgment, authored as a legible contract: a version-controlled rubric, a difficulty-graded curriculum, and a curated external knowledge base. The agent’s domain competence comes from those artifacts, not from weights and not from a blank harness, which is why the contract is the durable asset and the agent is its derivative.

AgentBuild builds the agent from that contract. The stage has a declared interface (curriculum, rubric, producer external knowledge base, base model handle, MCP tool inventory, edit boundary), an acceptance test (a rubric-driven LLM judge over the curriculum), a build step (a meta-optimizer LLM that

mutates the AUD assembly within the declared boundary), and two outputs (a versioned, A2A-packaged agent and a provenance trail). The build compiles the agent, not the scientist’s judgment.

Instantiating AgentBuild for Rietveld refinement of XRD data through GSAS-II and an MCP server gives the contract concrete SNR evidence. The construction run produces a usable Rietveld AUD, reaches an iteration 7 four-case P-strict milestone, and continues to plausible high-count LLZO refinements at the 4 hour frontier. The SNR holdout rows add a second lesson: the terminal AUD preserves strong scientific-reporting and trajectory behavior on reserved SNR cases, while the D1-D3 misses show where deterministic machine-checkable reporting needs a sharper interface. That interface is the front line where non-deterministic scientific narration first meets deterministic validation.

The remaining limitations define the next expansion targets. In the Rietveld setting, future work should extend beyond single-phase, SNR-focused refinement toward phase identification, multiphase refinement, phase-count detection, weak impurity modeling, and broader material and instrument classes. At the workflow-system level, future versions should harden identity propagation through MCP tool chains, support A2A endpoint multi-tenancy, stress-test rubrics under adversarial pressure, and bootstrap curricula in domains that lack an authored seed. Such explorations would make AgentBuild more useful by widening the kinds of scientist-authored contracts it can consume, evaluate, and turn into deployed agents while keeping the contract, rather than the generated agent, as the durable scientific asset.

ACKNOWLEDGMENTS

This work was supported by the U.S. Department of Energy, Office of Science, Office of Advanced Scientific Computing Research under Contract No. DE-SCL0000175, “A Testbed for Multi-Agent Autonomous Science: From Lab Bench to Supercomputer”. This research used resources of the Oak Ridge Leadership Computing Facility at the Oak Ridge National Laboratory, supported by the Office of Science of the U.S. Department of Energy under Contract No. DE-AC05-00OR22725. Claude (Anthropic) and ChatGPT (OpenAI) were used throughout this paper to assist with prose drafting, code generation, figure development, and literature search. All research ideas, experimental design, and conclusions are the authors’ own. The authors reviewed and take full responsibility for all content [29], [49].

REFERENCES

- [1] F. Suter, T. Coleman, İ. Altıntaş, R. M. Badia, B. Balis, K. Chard, I. Colonnelli, E. Deelman, P. Di Tommaso, T. Fahringer *et al.*, “A terminology for scientific workflow systems,” *Future Generation Computer Systems*, vol. 174, p. 107974, 2026.
- [2] O. Yildiz and T. Peterka, “Do large language models speak scientific workflows?” 2024. [Online]. Available: <https://arxiv.org/abs/2412.10606>
- [3] Z. Shao, P. Wang, Q. Zhu, R. Xu, J. Song, X. Bi, H. Zhang, M. Zhang, Y. K. Li, Y. Wu, and D. Guo, “DeepSeekMath: Pushing the limits of mathematical reasoning in open language models,” 2024, introduces Group Relative Policy Optimization (GRPO). [Online]. Available: <https://arxiv.org/abs/2402.03300>

- [4] DeepSeek-AI, D. Guo, D. Yang, H. Zhang, J. Song, R. Zhang, R. Xu, Q. Zhu, S. Ma, P. Wang, X. Bi, X. Zhang, X. Yu, Y. Wu, Z. F. Wu, Z. Gou, Z. Shao, Z. Li, Z. Gao, and A. Liu, "DeepSeek-R1: Incentivizing reasoning capability in LLMs via reinforcement learning," *Nature*, vol. 645, pp. 633–638, 2025, author list truncated; see arXiv for full DeepSeek-AI roster. [Online]. Available: <https://arxiv.org/abs/2501.12948>
- [5] B. H. Toby and R. B. Von Dreele, "GSAS-II: the genesis of a modern open-source all purpose crystallography software package," *Journal of Applied Crystallography*, vol. 46, no. 2, pp. 544–549, 2013.
- [6] Anthropic, "Model context protocol specification," <https://modelcontextprotocol.io/specification>, 2024, open protocol for LLM-tool integration; specification version 2025-11-25 (revision dated 2025-11-25 in the canonical schema repository at <https://github.com/modelcontextprotocol/specification>). Originally announced by Anthropic November 2024.
- [7] A2A Project, Google, and Linux Foundation, "Agent2agent (A2A) protocol specification," <https://a2a-protocol.org/latest/specification/>, 2025, open protocol for inter-agent communication; specification version 1.0.0 (announced by Google at Cloud Next on 2025-04-09; contributed to the Linux Foundation in June 2025; v0.3 released 2025-07-31). Canonical schema at <https://github.com/a2aproject/A2A>.
- [8] L. Zheng, W.-L. Chiang, Y. Sheng, S. Zhuang, Z. Wu, Y. Zhuang, Z. Lin, Z. Li, D. Li, E. P. Xing, H. Zhang, J. E. Gonzalez, and I. Stoica, "Judging LLM-as-a-judge with MT-bench and chatbot arena," in *Advances in Neural Information Processing Systems 36 (NeurIPS 2023)*, *Datasets and Benchmarks Track*, 2023. [Online]. Available: <https://arxiv.org/abs/2306.05685>
- [9] S. R. Wilkinson, M. Aloqalaa, K. Belhajjame, M. R. Crusoe, B. de Paula Kinoshita, L. Gadelha, D. Garijo, O. J. R. Gustafsson, N. Juty, S. Kanwal, F. Z. Khan, J. Köster, K. Peters-von Gehlen, L. Pouchard, R. K. Rannow, S. Soiland-Reyes, N. Soranzo, S. Sufi, Z. Sun, B. Vilne, M. A. Wouters, D. Yuen, and C. Goble, "Applying the FAIR principles to computational workflows," *Scientific Data*, vol. 12, p. 328, 2025.
- [10] R. Souza, A. Gueroudji, S. DeWitt, D. Rosendo, T. Ghosal, R. Ross, P. Balaprakash, and R. Ferreira da Silva, "PROV-AGENT: Unified provenance for tracking AI agent interactions in agentic workflows," in *Proceedings of the 21st IEEE International Conference on e-Science (eScience 2025)*, Chicago, IL, USA, 2025.
- [11] M. D. Wilkinson, M. Dumontier, I. J. Aalbersberg, G. Appleton, M. Axton, A. Baak, N. Blomberg, J.-W. Boiten, L. B. da Silva Santos, P. E. Bourne *et al.*, "The FAIR guiding principles for scientific data management and stewardship," *Scientific Data*, vol. 3, p. 160018, 2016.
- [12] M. Barker, N. P. Chue Hong, D. S. Katz, A.-L. Lamprecht, C. Martinez-Ortiz, F. Psomopoulos, J. Harrow, L. J. Castro, M. Gruenpeter, P. A. Martinez, and T. Honeyman, "Introducing the FAIR principles for research software," *Scientific Data*, vol. 9, no. 1, p. 622, 2022.
- [13] C. Goble, S. Cohen-Boulakia, S. Soiland-Reyes, D. Garijo, Y. Gil, M. R. Crusoe, K. Peters, and D. Schober, "FAIR computational workflows," *Data Intelligence*, vol. 2, no. 1-2, pp. 108–121, 2020.
- [14] S. Yao, J. Zhao, D. Yu, N. Du, I. Shafraan, K. Narasimhan, and Y. Cao, "ReAct: Synergizing reasoning and acting in language models," in *International Conference on Learning Representations (ICLR 2023)*, 2023. [Online]. Available: <https://arxiv.org/abs/2210.03629>
- [15] N. Shinn, F. Cassano, E. Berman, A. Gopinath, K. Narasimhan, and S. Yao, "Reflexion: Language agents with verbal reinforcement learning," in *Advances in Neural Information Processing Systems 36 (NeurIPS 2023)*, 2023. [Online]. Available: <https://arxiv.org/abs/2303.11366>
- [16] E. Deelman, K. Vahi, G. Juve, M. Rynge, S. Callaghan, P. J. Maechling, R. Mayani, W. Chen, R. Ferreira da Silva, M. Livny, and K. Wenger, "Pegasus, a workflow management system for science automation," *Future Generation Computer Systems*, vol. 46, pp. 17–35, 2015.
- [17] J. Köster and S. Rahmann, "Snakemake—a scalable bioinformatics workflow engine," *Bioinformatics*, vol. 28, no. 19, pp. 2520–2522, 2012.
- [18] P. Di Tommaso, M. Chatzou, E. W. Floden, P. P. Barja, E. Palumbo, and C. Notredame, "Nextflow enables reproducible computational workflows," *Nature Biotechnology*, vol. 35, no. 4, pp. 316–319, 2017.
- [19] M. R. Crusoe, S. Abeln, A. Iosup, P. Amstutz, J. Chilton, N. Tijanić, H. Ménager, S. Soiland-Reyes, B. Gavrilović, and C. Goble, "Methods included: Standardizing computational reuse and portability with the Common Workflow Language," *Communications of the ACM*, vol. 65, no. 6, pp. 54–63, 2022.
- [20] Y. Babuji, A. Woodard, Z. Li, D. S. Katz, B. Clifford, R. Kumar, L. Lacinski, R. Chard, J. M. Wozniak, I. Foster, M. Wilde, and K. Chard, "Parsl: Pervasive parallel programming in Python," in *Proceedings of the 28th International Symposium on High-Performance Parallel and Distributed Computing (HPDC '19)*. Phoenix, AZ, USA: Association for Computing Machinery, 2019, pp. 25–36.
- [21] R. Chard, Y. Babuji, Z. Li, T. Skluzacek, A. Woodard, B. Blaiszik, I. Foster, and K. Chard, "funcX: A federated function serving fabric for science," in *Proceedings of the 29th International Symposium on High-Performance Parallel and Distributed Computing (HPDC '20)*. Stockholm, Sweden: Association for Computing Machinery, 2020, pp. 65–76.
- [22] E. Afgan, D. Baker, B. Batut, M. van den Beek, D. Bouvier, M. Čech, J. Chilton, D. Clements, N. Coraor, B. A. Grüning, A. Guerler, J. Hillman-Jackson, S. Hiltmann, V. Jalili, H. Rasche, N. Soranzo, J. Goecks, J. Taylor, A. Nekrutenko, and D. Blankenberg, "The Galaxy platform for accessible, reproducible and collaborative biomedical analyses: 2018 update," *Nucleic Acids Research*, vol. 46, no. W1, pp. W537–W544, 2018.
- [23] J. Goecks, A. Nekrutenko, and J. Taylor, "Galaxy: a comprehensive approach for supporting accessible, reproducible, and transparent computational research in the life sciences," *Genome Biology*, vol. 11, no. 8, p. R86, 2010.
- [24] O. Khattab, A. Singhvi, P. Maheshwari, Z. Zhang, K. Santhanam, S. Vardhamanan, S. Haq, A. Sharma, T. T. Joshi, H. Moazam, H. Miller, M. Zaharia, and C. Potts, "DSPy: Compiling declarative language model calls into self-improving pipelines," in *International Conference on Learning Representations (ICLR 2024)*, 2024. [Online]. Available: <https://arxiv.org/abs/2310.03714>
- [25] L. A. Agrawal, S. Tan, D. Soylu, N. Ziemis, R. Khare, K. Opsahl-Ong, A. Singhvi, H. Shandilya, M. J. Ryan, M. Jiang, C. Potts, K. Sen, A. G. Dimakis, I. Stoica, D. Klein, M. Zaharia, and O. Khattab, "GEPa: Reflective prompt evolution can outperform reinforcement learning," in *International Conference on Learning Representations (ICLR 2026, Oral)*, 2025. [Online]. Available: <https://arxiv.org/abs/2507.19457>
- [26] B. Romera-Paredes, M. Barekatin, A. Novikov, M. Balog, M. P. Kumar, E. Dupont, F. J. R. Ruiz, J. S. Ellenberg, P. Wang, O. Fawzi, P. Kohli, and A. Fawzi, "Mathematical discoveries from program search with large language models," *Nature*, vol. 625, pp. 468–475, 2024.
- [27] Y. J. Ma, W. Liang, G. Wang, D.-A. Huang, O. Bastani, D. Jayaraman, Y. Zhu, L. Fan, and A. Anandkumar, "Eureka: Human-level reward design via coding large language models," in *International Conference on Learning Representations (ICLR)*, 2024. [Online]. Available: <https://arxiv.org/abs/2310.12931>
- [28] H. M. Rietveld, "A profile refinement method for nuclear and magnetic structures," *Journal of Applied Crystallography*, vol. 2, no. 2, pp. 65–71, 1969.
- [29] Anthropic, "Claude," <https://www.anthropic.com>, 2026, accessed: 2026.
- [30] A. Al-Najjar, N. S. V. Rao, C. A. Bridges, S. Dai, and A. Walters, "Autonomous electrochemistry platform with real-time normality testing of voltammetry measurements using ML," in *Proceedings of the 2024 IEEE 20th International Conference on e-Science (e-Science)*. IEEE, 2024, pp. 1–10, oRNL ACL system paper; Pyro RPC framework and ML normality testing.
- [31] Oak Ridge National Laboratory, "An autonomous chemistry lab for accelerated materials discovery and innovation," <https://www.ornl.gov/project/autonomous-chemistry-lab-accelerated-materials-discovery-and-innovation>, 2022, accessed: 2026-06-08.
- [32] A. Al-Najjar, N. S. V. Rao, C. A. Bridges, and S. Dai, "Cross-facility orchestration of electrochemistry experiments and computations," in *Workshops of the International Conference on High Performance Computing, Network, Storage, and Analysis (SC-W 2023)*. New York, NY, USA: ACM, Nov. 2023, pp. 2118–2125.
- [33] C. Engelmann, O. Kuchar, S. Boehm, M. J. Brim, T. Naughton, S. Somnath, S. Atchley, J. Lange, B. Mintz, and E. Arenholz, "The INTERSECT open federated architecture for the laboratory of the future," in *Communications in Computer and Information Science (CCIS): Accelerating Science and Engineering Discoveries Through Integrated Research Infrastructure for Experiment, Big Data, Modeling and Simulation*, ser. Communications in Computer and Information Science, vol. 1690. Cham: Springer, Aug. 2022, pp. 173–190, 18th Smoky Mountains Computational Sciences & Engineering Conference (SMC) 2022, August 24–25, 2022.

- [34] R. Souza, T. Poteet, B. Etz, D. Rosendo, A. Gueroudji, W. Shin, P. Balaprakash, and R. Ferreira da Silva, "LLM agents for interactive workflow provenance: Reference architecture and evaluation methodology," in *Proceedings of the SC '25 Workshops of the International Conference for High Performance Computing, Networking, Storage and Analysis (WORKS25)*, St. Louis, MO, USA, 2025.
- [35] M. Sim, M. G. Vakili, F. Strieth-Kalthoff, H. Hao, R. J. Hickman, S. Miret, S. Pablo-García, and A. Aspuru-Guzik, "ChemOS 2.0: An orchestration architecture for chemical self-driving laboratories," *Matter*, vol. 7, no. 9, pp. 2959–2977, 2024.
- [36] R. D. Lewis, T. S. Ginsburg, D. Ozgulbas, C. Stone, A. Stroka, A. Cleary, I. T. Foster, and N. Paulson, "MADSci: A modular python-based framework to enable autonomous science," *Journal of Open Source Software*, vol. 11, no. 119, p. 9416, 2026, argonne MADSci framework: <https://github.com/AD-SDL/MADSci>.
- [37] L. Ward, J. G. Pauloski, V. Hayot-Sasson, Y. Babuji, A. Brace, R. Chard, K. Chard, R. Thakur, and I. Foster, "Employing artificial intelligence to steer exascale workflows with Colmena," *The International Journal of High Performance Computing Applications*, vol. 39, no. 1, pp. 52–64, 2025.
- [38] R. Vescovi, T. Ginsburg, K. Hippe, D. Ozgulbas, C. Stone, A. Stroka, R. Butler, B. Blaiszik, T. Brettin, K. Chard, M. Hereld, A. Ramanathan, R. Stevens, A. Vriza, J. Xu, Q. Zhang, and I. Foster, "Towards a modular architecture for science factories," *Digital Discovery*, vol. 2, no. 6, pp. 1980–1998, 2023.
- [39] A. M. Bran, S. Cox, O. Schilter, C. Baldassari, A. D. White, and P. Schwaller, "Augmenting large language models with chemistry tools," *Nature Machine Intelligence*, vol. 6, no. 5, pp. 525–535, 2024, chem-Crow LLM-with-tools chemistry agent.
- [40] D. A. Boiko, R. MacKnight, B. Kline, and G. Gomes, "Autonomous chemical research with large language models," *Nature*, vol. 624, no. 7992, pp. 570–578, 2023, coscientist GPT-4 driven autonomous chemistry agent.
- [41] N. J. Szymanski, B. Rendy, Y. Fei, R. E. Kumar, T. He, D. Milsted, M. J. McDermott, M. Gallant, E. D. Cubuk, A. Merchant, H. Kim, A. Jain, C. J. Bartel, K. Persson, Y. Zeng, and G. Ceder, "An autonomous laboratory for the accelerated synthesis of inorganic materials," *Nature*, vol. 624, no. 7990, pp. 86–91, 2023, a-Lab autonomous materials synthesis platform.
- [42] J. Gottweis, W.-H. Weng, A. Daryin, T. Tu, A. Palepu, P. Sirkovic, A. Myaskovsky, F. Weissenberger, K. Rong, R. Tanno, K. Saab, D. Popovici, J. Blum, F. Zhang, K. Chou, A. Hassidim, B. Gokturk, A. Vahdat, P. Kohli, Y. Matias, A. Carroll, K. Kulkarni, N. Tomasev, Y. Guan, V. Dhillon, E. D. Vaishnav, B. Lee, T. R. D. Costa, J. R. Penadés, G. Peltz, Y. Xu, A. Pawlosky, A. Karthikesalingam, and V. Natarajan, "Towards an AI co-scientist," 2025. [Online]. Available: <https://arxiv.org/abs/2502.18864>
- [43] C. Lu, C. Lu, R. T. Lange, J. Foerster, J. Clune, and D. Ha, "The AI scientist: Towards fully automated open-ended scientific discovery," 2024, sakana AI technical report. [Online]. Available: <https://arxiv.org/abs/2408.06292>
- [44] Y. Ozaki, Y. Suzuki, T. Hawaii, K. Saito, M. Onishi, and K. Ono, "Automated crystal structure analysis based on blackbox optimisation," *npj Computational Materials*, vol. 6, no. 1, p. 75, 2020, bBO-Rietveld implementation and seed data: <https://github.com/quantumbeam/BBO-Rietveld>.
- [45] T. Akiba, S. Sano, T. Yanase, T. Ohta, and M. Koyama, "Optuna: A next-generation hyperparameter optimization framework," in *Proceedings of the 25th ACM SIGKDD International Conference on Knowledge Discovery & Data Mining*, 2019, pp. 2623–2631.
- [46] N. J. Szymanski, C. J. Bartel, Y. Zeng, M. Diallo, H. Kim, and G. Ceder, "Adaptively driven X-ray diffraction guided by machine learning for autonomous phase identification," *npj Computational Materials*, vol. 9, no. 1, p. 31, 2023, adaptive-XRD release with Aeris UAI driver: <https://github.com/njszym/Adaptive-XRD>.
- [47] P. M. Maffettone, L. Banko, P. Cui, Y. Lysogorskiy, M. A. Little, D. Olds, A. Ludwig, and A. I. Cooper, "Crystallography companion agent for high-throughput materials discovery," *Nature Computational Science*, vol. 1, no. 4, pp. 290–297, 2021.
- [48] Y. Fei, M. J. McDermott, C. L. Rom, S. Wang, and G. Ceder, "Dara: Automated multiple-hypothesis phase identification and refinement from powder X-ray diffraction," *Chemistry of Materials*, vol. 38, no. 3, pp. 1364–1376, 2026.
- [49] OpenAI, "ChatGPT," <https://www.openai.com>, 2026, accessed: 2026.